Structure of Compounds in the $Sr_{1-3x/2}Ce_xTiO_3$ Homologous Series

Rick Ubic,*,† Ganesanpotti Subodh,‡ Mailadil T. Sebastian,‡ Delphine Gout,§ and Thomas Proffen§

Department of Materials Science & Engineering, Boise State University, Boise, Idaho, Materials and Minerals Division, National Institute for Interdisciplinary Science and Technology, Trivandrum 695 019, India, and Los Alamos Neutron Science Center, Los Alamos, New Mexico

Received December 21, 2007. Revised Manuscript Received February 19, 2008

Four compositions in the $Sr_{1-3x/2}Ce_xTiO_3$ homologous series, corresponding to $x = 0.1333$, 0.1667, 0.25, and 0.4, have been produced by conventional solid-state processing. The structure of these compounds was analyzed by X-ray, electron, and neutron diffraction. While no superlattice can be observed via X-ray diffraction, both electron and neutron diffraction show evidence of a noncubic supercell caused by antiphase tilting of oxygen octahedra. The most likely space group is $R\bar{3}c$, corresponding to an $a^-a^-a^-$ tilt system, except for the composition $x = 0.4$, for which an even more complex superstructure is observed. The degree of tilt increases with increasing x.

Introduction

Developments in microwave wireless communications over the past 20 years or so have pushed technological advances in the field of perovskite engineering. In particular, complex perovskites have received widespread interest in the industry; however, the number of low-loss ceramic materials with high dielectric constant ($\epsilon_r > 100$) remains very small. Indeed, the development of microwave ceramics with high dielectric constant and good thermal stability together with small dielectric loss is a challenging problem in the area of microwave dielectric resonator materials research.

Many electroceramics are based on or related to the perovskite crystal structure. Perovskites can be described by the general formula ABO_3, and complex perovskites of the type $A(B'B'')O_3$are now well-established materials for microwave applications because of their high quality factors (Qf) and low temperature coefficients of resonant frequency (τ_f). These materials usually have divalent species on the A-site, although some newer compositions incorporate trivalent rare-earth cations on the A-site with charge compensation conferred by the simultaneous incorporation of a trivalent species like Al^{3+} on the B-site, e.g., $(Ca_{1-x}Nd_x)(Ti_{1-x}Al_x)O_3$. In the Ce-doped $SrTiO_3$ system, it has been proposed[1] that charge compensation occurs simply via A-site vacancy formation, with Ce^{3+} dopants occupying Sr^{2+} sites and creating A-site vacancies via the reaction:

$$Ce_2O_3 \xrightarrow{SrTiO_3} 2Ce_{Sr}^{\bullet\bullet} + V_{Sr}^{''} + 3O_O^x$$

These materials typically have dielectric constants in the 113−185 range and quality factors from 6000 to 11 000. As such, they are promising, relatively inexpensive, Pb-free candidates for high-permittivity applications (e.g., cellular handsets) in the wireless telecommunications field.

Recently, Sreemoolanadhan et al.[2] reported the microwave dielectric properties of ceramics in the $BaO-2CeO_2-nTiO_2$ system with reasonably good microwave dielectric properties. Bamberger et al.[3] had previously reported the existence of the compound $Sr_2Ce_2Ti_5O_{16}$ and a series of solid solutions of the type $Sr_{2+n}Ce_2Ti_{5+n}O_{16+3n}$ ($n \leq 7$); however, the crystal structure and phase purity of these compounds were not well-established. It was determined in previous work[1] that such ceramics prepared via the route described by Bamberger et al.[3] contain Ce^{3+} rather than Ce^{4+}, so the formula is more correctly written as $Sr_{2+n}Ce_2Ti_{5+n}O_{15+3n}$ or more simply $Sr_{1-3x/2}Ce_xTiO_3$, where $x = 2/(n + 5)$.

The structure of $Sr_{1-3x/2}Ce_xTiO_3(0.1333 \leq x \leq 0.4)$ has recently been reported as cubic, $Pm\bar{3}m$, on the basis of X-ray diffraction data[1] and vibrational spectroscopy work.[4] The similar $Sr_{1-3x/2}La_xTiO_3$ system was previously investigated by Howard et al.,[5] who found that at room temperature antiphase octahedral tilting about one axis drives a $Pm\bar{3}m \rightarrow I4/mcm$ transition at $x \approx 0.2$, and cation ordering drives a further transition to $Cmmm$ at $x \geq 0.55$. The same group[6] later investigated the specific $Sr_{0.1}La_{0.6}TiO_3$ ($x = 0.6$) composition and found two polymorphs (one ordered in $P4/mmm$ and another disordered in $Pm\bar{3}m$) that both underwent the same tilt transition below ≈290−300 °C to yield symmetry changes $P4/mmm \rightarrow Cmmm$ and $Pm\bar{3}m \rightarrow$

* Corresponding author. Tel: +1 208 426 2309. Fax: +1 208 426 2470. E-mail: RickUbic@BoiseState.edu.
† Boise State University.
‡ Institute of Interdisciplinary Sciences and Technology.
§ Los Alamos Neutron Science Center.

(1) Subodh, G.; James, J.; Sebastian, M. T.; Paniago, R.; Dias, A.; Moreira, R. L. *Chem. Mater.* **2007**, *19*, 4077.
(2) Sreemoolanadhan, H.; Sebastian, M. T.; Ratheesh, R.; Blachnik, R.; Woehlecke, M.; Schneider, B.; Neumann, M.; Mohanan, P. *J. Solid State Chem.* **2004**, *177*, 3995.
(3) Bamberger, C. E.; Haverlock, T. J.; Kopp, O. C. *J. Am. Ceram. Soc.* **1994**, *77*, 1659.
(4) Moreira, R. L.; Lobo, R.P.S.M.; Subodh, G.; Sebastian, M. T.; Matinaga, F. M.; Dias, A. *Chem. Mater.* **2007**, *19*, 6548.
(5) Howard, C. J.; Lumpkin, G. R.; Smith, R. I.; Zhang, Z. J. *Solid State Chem.* **2004**, *177*, 2726.
(6) Howard, C. J.; Zhang, Z.; Carpenter, M. A.; Knight, K. S. *Phys. Rev. B* **2007**, *76*, 054108.

10.1021/cm703659f CCC: $40.75
Published on Web 04/05/2008

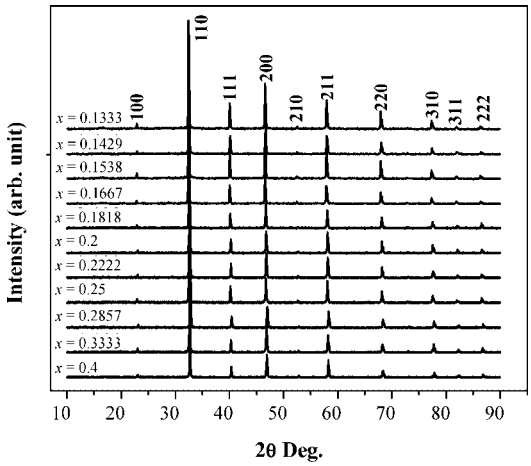

Figure 1. XRD patterns for $Sr_{1-3x/2}Ce_xTiO_3$ compositions corresponding to $0.1333 \leq x \leq 0.4$ sintered at 1400 °C ($0.1333 \leq x \leq 0.1538$), 1375 °C ($0.1667 \leq x \leq 0.3333$), and 1300 °C ($x = 0.4$) (after ref 1).

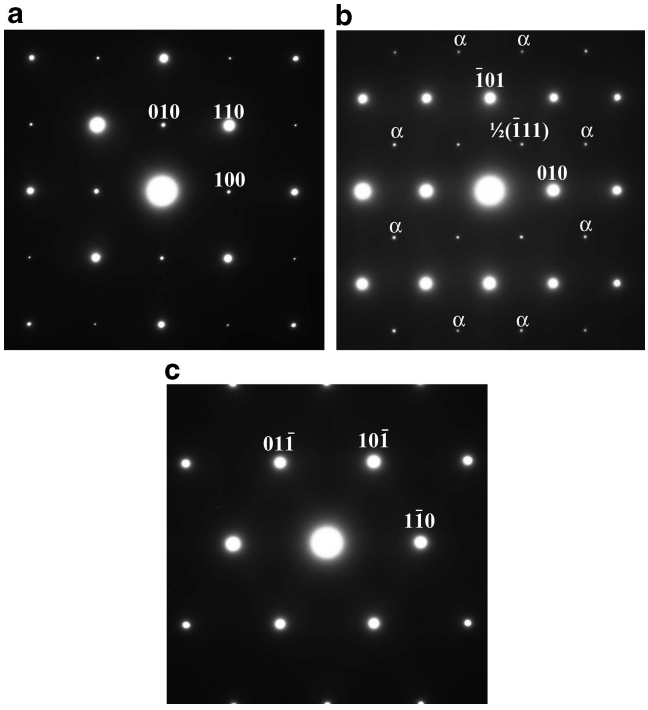

Figure 2. Selected-area electron diffraction patterns from grains of the $x = 0.25$ composition corresponding to (a) [001], (b) [101], and (c) [111] pseudocubic directions. Superlattice reflections are denoted with an α in part b.

I4/mcm. In neither work was electron diffraction used as a means of determining the tilt system. In the present investigation, electron and neutron diffraction were employed to investigate the crystal symmetry of the $Sr_{1-3x/2}Ce_xTiO_3$ system.

Experimental Methods

$Sr_{1-3x/2}Ce_xTiO_3$ ($0.1333 \leq x \leq 0.4$) ceramics were prepared by a conventional solid-state ceramic route. High-purity $SrCO_3$ and TiO_2 (99.9+%, Aldrich Chemical Co., Inc., Milwaukee, WI) and CeO_2 (99.99%, Indian Rare Earth Ltd., Udyogamandal, India) were used as the starting materials. Stoichiometric amounts of powder mixtures were ball-milled in distilled water medium using yttria-stabilized zirconia balls in a plastic container for 24 h. The slurry was dried, ground, and calcined at 1100 °C for 5 h. The calcined

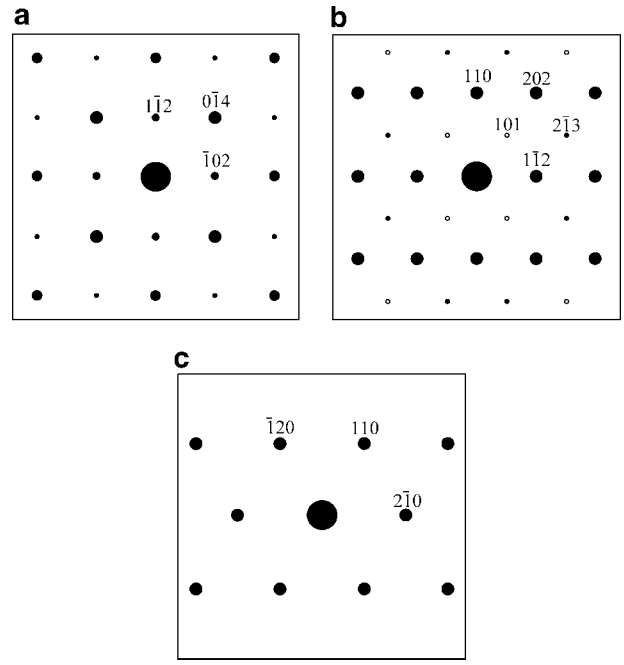

Figure 3. Schematic indexing, according to the proposed $R\bar{3}c$ structure, of the SADPs in Figure 2. Solid circles represent allowed reflections, while open circles represent reflections present via double diffraction. (a) [241], (b) [$\bar{1}$11], (c) [001].

material was ground into a fine powder and divided into different batches for sintering trials. Around 4 wt% of polyvinyl alcohol (PVA) (molecular weight 22 000, 88% hydrolyzed, BDH Laboratory Supplies) was added to the dried powders, which were then again ground into fine powder. Cylindrical pellets of about 1–2 mm height and about 14 mm diameter were made by applying a pressure of 100 MPa. These compacts were then fired at 600 °C for 30 min to burn the binder out before sintering at temperatures ranging from 1300 to 1400 °C. Crystal structure and phase purity of the powdered samples were studied by X-ray diffraction (XRD) using Ni-filtered Cu Kα radiation (D/MAX, Rigaku).

Samples for transmission electron microscopy (TEM) were prepared by thinning pellets to electron transparency by conventional ceramographic techniques followed by ion thinning (model 600, Gatan, Pleasanton, CA) to electron transparency for observation in the TEM (JEM-2100 HR, JEOL).

Time-of-flight (ToF) neutron diffraction data were collected for $Sr_{1-3x/2}Ce_xTiO_3$ ($x = 0.1333$, 0.1667, 0.25, 0.4) on the neutron powder diffractometer (NPDF) at the Manuel Lujan Neutron Scattering Center of Los Alamos National Laboratory. This instrument is a high-resolution powder diffractometer located at flight path 1, 32 m from the spallation neutron target. Powder samples were contained in a vanadium can 0.95 cm in diameter. Absorption was not a problem. The data were collected at room temperature (300 K) using the 148°, 119°, 90°, and 46° banks, which cover a *d*-spacing range from 0.12 to 7.2 Å. Unit cell parameters, atomic positions, and isotropic displacement parameters (IDPs) were refined for the various compositions using the JANA2006 program.[7] An occupational restriction on Sr and Ce was used that maintains the sum of the two fractional occupations at the total value for the A-site expected from stoichiometry.

(7) Petricek, V., Dusek, M., Palatinus, *Jana2006. The Crystallographic Computing System*; Institute of Physics: Praha, Czech Republic, 2006.

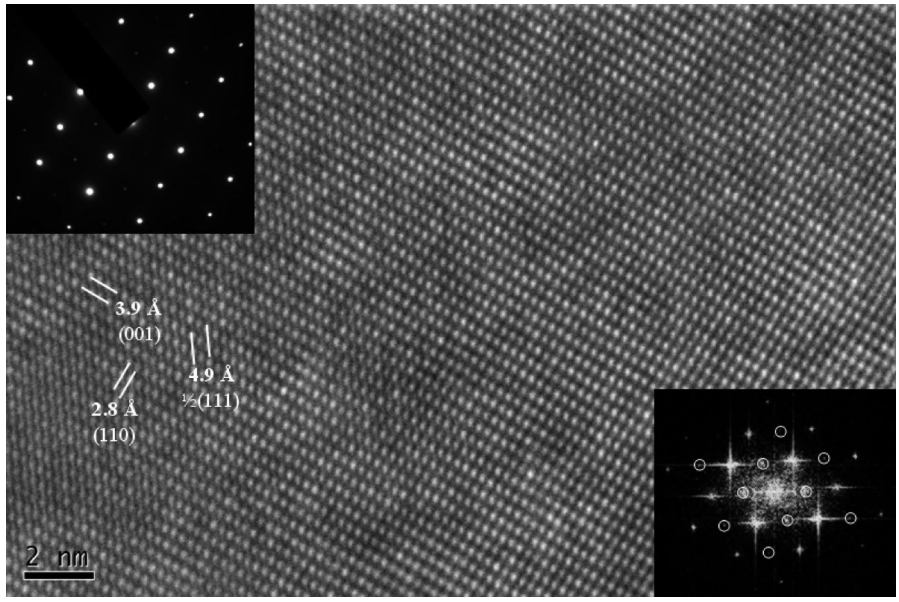

Figure 4. High-resolution image of the $x = 0.25$ composition parallel to the pseudocubic [110]. The lower-right inset is a Fourier transform of the image with superlattice spots circled.

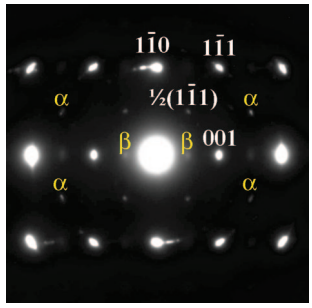

Figure 5. Pseudocubic [110] selected area diffraction pattern of the $x = 0.4$ composition with α and β superlattice reflections indicated.

Results and Discussion

All compositions tested appeared to be single-phase, essentially consisting of a solid solution of $SrTiO_3$ and $Ce_2Ti_3O_9$. The $Ce_2Ti_3O_9$ compound has been variously reported as either an undistorted perovskite with *Pm3m* symmetry[8] or a doubled perovskite with *Pmmm* symmetry.[9] The oxygen-deficient versions of this phase are also typically reported in orthorhombic settings. Figure 1 shows XRD patterns for $Sr_{1-3x/2}Ce_xTiO_3$ compositions corresponding to $0.1333 \leq x \leq 0.4$ sintered at 1400 °C ($0.1333 \leq x \leq 0.1538$), 1375 °C ($0.1667 \leq x \leq 0.3333$), and 1300 °C ($x = 0.4$). Each pattern can be indexed unambiguously according to a simple cubic unit cell, the dimensions of which, predictably, approach those of pure $SrTiO_3$ ($a = 3.901$ Å) as x decreases.

Figure 2 shows selected area electron diffraction patterns (SADPs) parallel to the pseudocubic directions [001], [101], and [111] in an $x = 0.25$ sample. Both the [001] and [111] patterns can be indexed unambiguously according to a primitive simple cubic perovskite unit cell; however, faint superlattice reflections in the [101] pattern cannot be explained by this structure. The extra reflections closest to the central transmitted spot correspond to ½{111}, a fact that clearly indicates that the lattice constant must be doubled and the symmetry lowered. Furthermore, the pattern cannot be explained using Yoshii's $Ce_2Ti_3O_9$ model[9] in *Pmmm*, although both the [001] and [111] can. Similar patterns were obtained for every composition examined. In addition, every ⟨110⟩ pattern observed in this system contained α superlattice reflections, making it very doubtful whether antiphase tilting occurs about only a single axis, as in the *I4/mcm* model ($a^0a^0c^-$ tilt system) of $Sr_{1-3x/2}La_xTiO_3$ published by Howard et al.[5] It is much more probable that such tilting occurs about two or even three pseudocubic axes. In addition, some of the superlattice reflections observed here would be forbidden even by double diffraction in *I4/mcm*. The alternative *Cmmm* symmetry, also reported for $Sr_{1-3x/2}La_xTiO_3$ by Howard et al.,[5] allows tilting about two axes, but it would also allow {110} reflections, which are never observed even for $x = 0.4$ Similarly, 001 and 021 spots would be expected in the [100] and/or [010] zones, but these are never observed except for when $x = 0.4$.

Doubling the unit cell parameter such that $a = 7.8$ Å, all three patterns can be indexed consistently by a face-centered cubic cell. Both ⟨001⟩ and ⟨111⟩ patterns are consistent in showing no ½{odd, odd, even} γ-type superlattice reflections, confirming the absence of in-phase octahedral tilts. On the other hand, every ⟨110⟩ pattern observed consistently shows a set of ½{odd, odd, odd} α-type reflections, confirming the presence of antiphase octahedral tilts about at least two, and possibly three, pseudocubic axes.[10]

With this in mind, tilt systems $a^0b^-c^-$ (space group *A2/m*), $a^0b^-b^-$ (space group *Imcm*), $a^-b^-c^-$ (space group $P\bar{1}$), $a^-b^-b^-$ (space group *I2/a*), and $a^-a^-a^-$ (space group $R\bar{3}c$) must be considered. In the case of the doubly tilted monoclinic *A2/m* (12) structure, all the observed α superlattice reflections, as well as the ½{111}, would be allowed, but some β-type reflections would also be allowed and are

(8) Leonov, A. I.; Piryutko, M. M.; Keler, E. K. *Bull. Acad. Sci. (USSR), Div. Chem. Sci.* **1966**, *5*, 756.
(9) Yoshii, K. *J. Alloys Compd.* **2000**, *305*, 72.
(10) Glazer, A. M. *Acta Crystallogr.* **1975**, *A31*, 756.

Table 1. Unit-Cell Parameters and Refinement Results for $Sr_{1-3x/2}Ce_xTiO_3$ at Room Temperature

	$x = 0.1333$	$x = 0.1667$	$x = 0.25$	$x = 0.4$
refined cell parameters (Å)	$a = b = 5.5091(2)$ $c = 13.5071(3)$	$a = b = 5.5062(2)$ $c = 13.4989(3)$	$a = b = 5.5005(2)$ $c = 13.4797(3)$	$a = b = 5.4860(2)$ $c = 13.4539(3)$
x position for the O[a]	0.5108(2)	0.5137(2)	0.5184(2)	0.5237(3)
angle of tilt, deg	1.2	1.5	2.0	2.6
Sr/Ce U_{iso}	0.008(1)	0.008(1)	0.008(1)	0.008(1)
Ti U_{iso}	0.006(1)	0.006(1)	0.007(1)	0.007(1)
O U_{iso}	0.0114(4)	0.0119(5)	0.0137(5)	0.0162(6)
$[Ce^{4+}]/[Ce_{total}]$[b]	0.03	0.05	0.06	0.10
Sr occupation refined/expected	0.795(7)/0.8	0.744(6)/0.75	0.601(7)/0.625	0.352(5)/0.4
Ce occupation refined/expected	0.133/0.133	0.167/0.166	0.269/0.25	0.445/0.4
Sr/Ce−O average bond length (Å)	2.7557	2.7544	2.7516	2.7457
Ti−O average bond length (Å)	1.9493	1.9488	1.9477	1.9447
Sr−O bond valence sum	1.7132	1.6154	1.3258	0.7988
Ce−O bond valence sum	0.3141	0.3964	0.6487	1.1041
Ti−O bond valence sum	4.1736	4.1793	4.1917	4.2258
overall GOF/Rwp	1.94/3.77%	2.07/3.90%	2.18/4.46%	11.43/5.16%

[a] Sr and Ce in 0, 0, ¼; Ti in 0, 0, 0; and O in x, 0, ¼. [b] From ref 1.

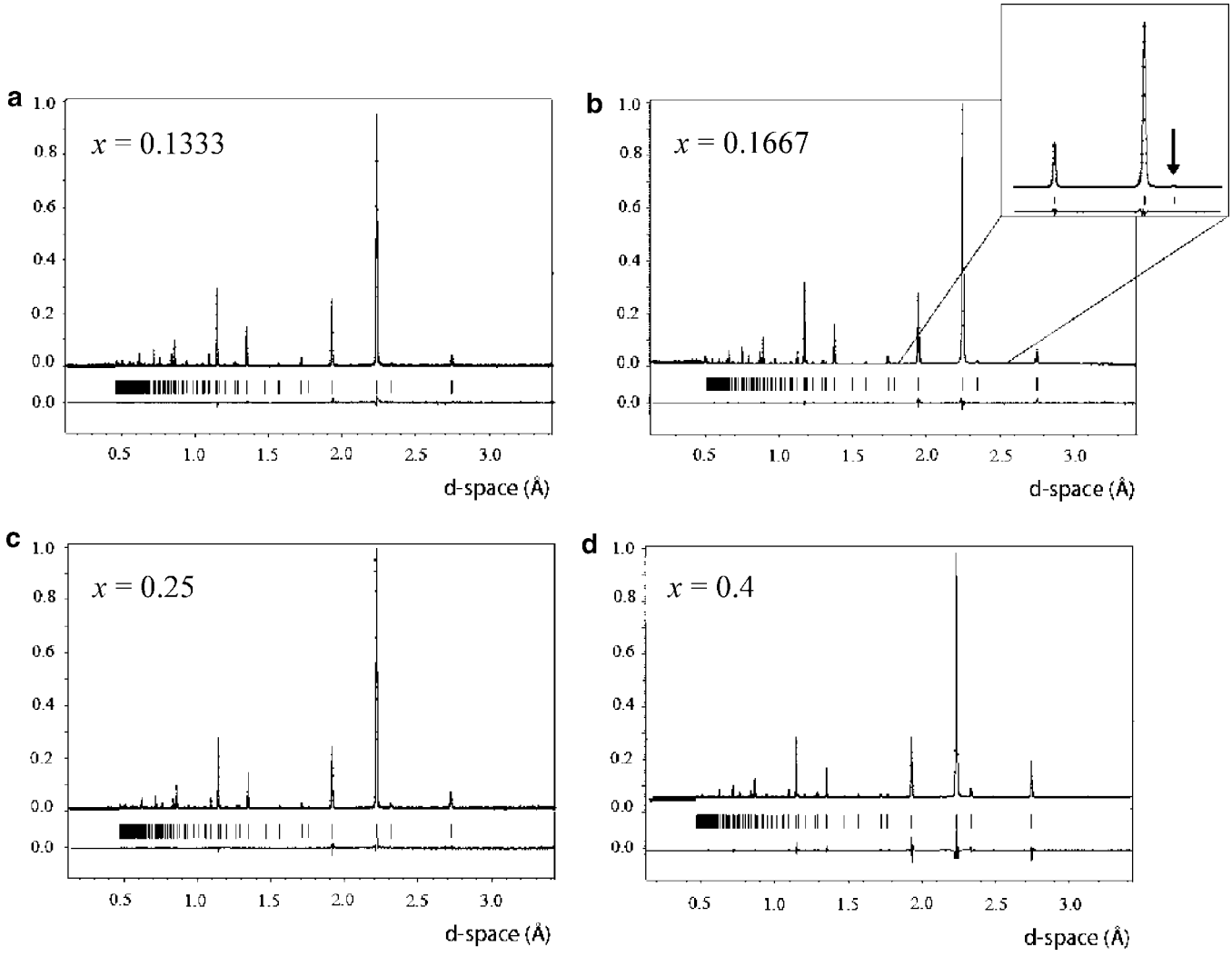

Figure 6. ToF neutron powder diffraction pattern for *d*-spacings between 0.5 and 3 Å for $Sr_{1-3x/2}Ce_xTiO_3$ ($x = 0.1333$, 0.1667, 0.25, 0.4) taken from data obtained with the 46° bank detectors. Observed data are represented by crosses; calculated results are represented by the line. The intensity scale uses arbitrary units. The difference curve is illustrated on the same scale. The arrow in the inset of b shows, as an example, a weak superlattice reflection at ≈2.35 Å corresponding to the pseudocubic ½{311}.

never observed except for when $x = 0.4$. Similarly, {011} reflections would also be allowed in *A*2/*m* but are never observed. The doubly tilted tetragonal *Imcm* model only allows some of the observed α reflections to appear via double diffraction, and so seems a doubtful choice. The triply tilted model in $P\bar{1}$ (2) also fails, as fundamental {100} type reflections, for example, are missing from diffraction patterns. Furthermore, the triply tilted *I*2/*a* (*C*2/*c*, 15) model does not work, as 101 or 011 reflections, both of which are forbidden in this space group, would be necessary to consistently explain the observed ⟨100⟩ and ⟨101⟩ pseudocubic patterns. Only $R\bar{3}c$, corresponding to antiphase tilts of equal

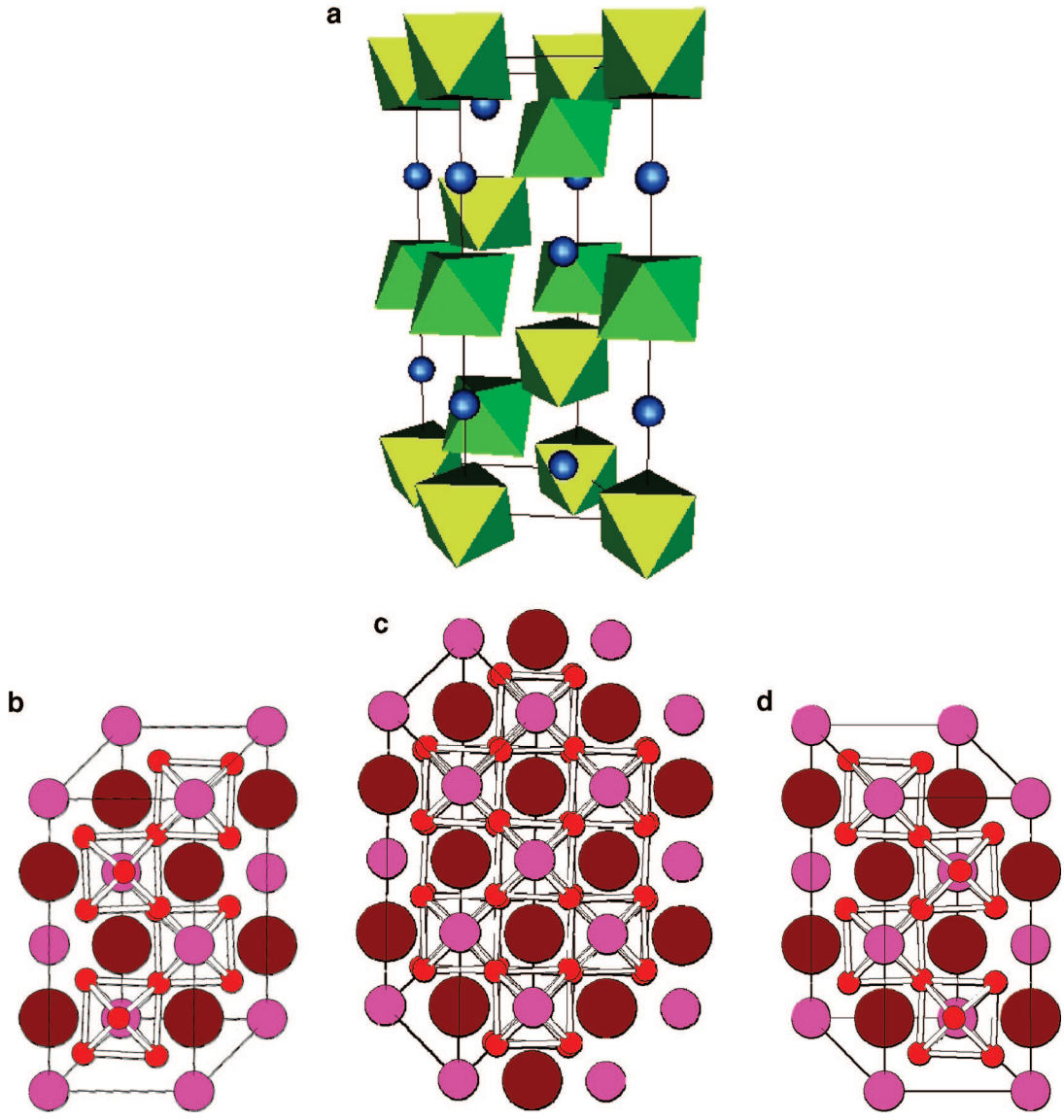

Figure 7. Unit cell of the $x = 0.25$ composition. In part a, the oxygen octahedra and Sr/Ce atoms are shown, but the oxygen ions at the octahedral apexes have been removed for clarity. With such a small (2°) tilt angle, the antiphase tilting is not obvious to the unaided eye in part a, but it is more apparent in parts b−d, which represent the unit cell as viewed along [4$\bar{2}\bar{1}$], [22$\bar{1}$], and [241], parallel to the pseudocubic [100], [010], and [001], respectively.

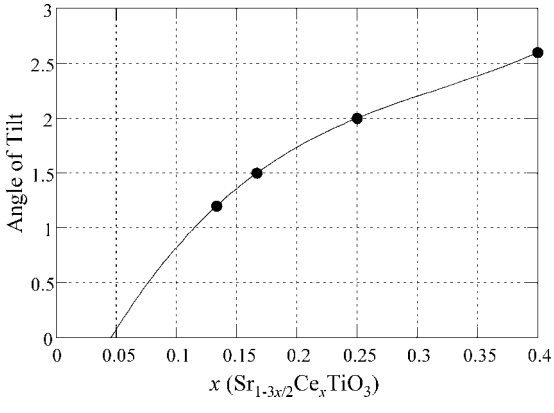

Figure 8. Angle of octahedral tilt vs composition. The superstructure should vanish for $x \leq 0.05$.

magnitude about each pseudocubic axis, is able to consistently index all the observed diffraction patterns, with the [001], [101], and [111] pseudocubic patterns corresponding to [241], [1$\bar{1}$1], and [001], respectively. Figure 3 shows schematics of the same patterns in Figure 2 but indexed according to a trigonal unit cell in $R\bar{3}c$, which corresponds to an $a^-a^-a^-$ tilt system. In such a tilt system, which is equivalent to the octahedra rotating about the cubic ⟨111⟩ triad axis, it is found empirically that the octahedra are flattened down their rotation axis.[11]

Figure 4 is a high-resolution image of the $x = 0.25$ composition parallel to a pseudocubic ⟨110⟩. The Fourier transform of the image appears in the inset and clearly demonstrates the existence of a noncubic superlattice. The pseudocubic {100} spacing measures consistently at about 3.9 Å from the image, in agreement with the XRD data (Figure 1). The measured {110} spacing (2.8 Å) is close to what one would expect for such a cubic crystal; however, the {111} spacing appears stretched. For a cubic crystal with a lattice constant of 3.9 Å, one would expect a {111} spacing of 2.3 Å. A simply doubled {111} would then be about 4.5

(11) Howard, C. J.; Kennedy, B. J.; Chakoumakos, B. C. *J. Phys.: Condens. Matter* **2000**, *12*, 349.

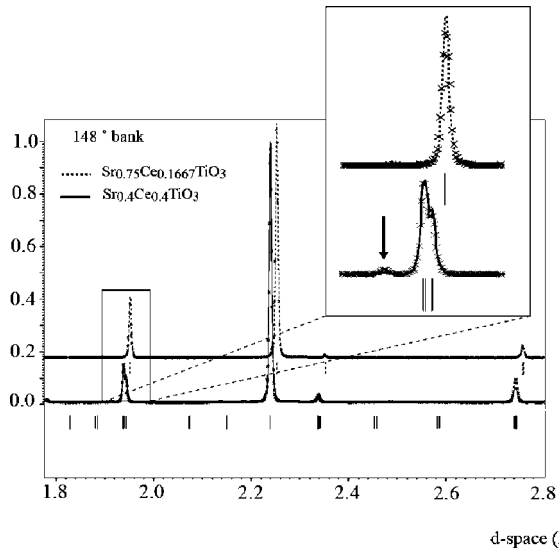

Figure 9. ToF neutron powder diffraction patterns for *d*-spacings between 1.8 and 2.8 Å for $Sr_{0.75}Ce_{0.1667}TiO_3$ (top dashed curve) and $Sr_{0.4}Ce_{0.4}TiO_3$ (bottom solid curve) taken from data obtained with the 148° bank detectors. Observed data are represented by crosses; calculated results are represented by the lines. The intensity scale uses arbitrary units. The tick marks represent the positions of peaks in space group $R\bar{3}c$ for $Sr_{0.75}Ce_{0.1667}TiO_3$ and *Cmmm* for $Sr_{0.4}Ce_{0.4}TiO_3$, respectively. The inset corresponds to an enlarged region of the *d*-spacing between 1.9 and 2.0 Å (see the text for additional details).

Å, but the ½{111} measured on this image is closer to 4.9 Å, indicating a stretch along a pseudocubic ⟨111⟩ (trigonal [001]), which would suggest a lowering of the symmetry to trigonal (and a trigonal *c*-axis of about 13.5 Å).

Hayward et al.[12] reported a $Pm\bar{3}m \rightarrow R\bar{3}c$ transformation in $NdAlO_3$ upon cooling below 540 °C brought about by an $a^-a^-a^-$ octahedral distortion. Similar distortions have been noted for high-temperature $LaMnO_3$[13–16] and $LaGaO_3$.[17–19] It is presumed here that at a sufficiently low value of x ($x < 0.1333$), the structural distortion in $Sr_{1-3x/2}Ce_xTiO_3$ would vanish completely and the $Pm\bar{3}m$ symmetry of pure $SrTiO_3$ would again be expressed.

The tolerance factor (t) for the perovskite crystal structure, given by equation 1, where R_A, R_B, and R_O are the radii of the A- and B-site ions and the O^{2-}-ion, respectively, indicates the stability of the perovskite structure for a given set of ions.

$$t = (R_A + R_O)/\sqrt{2}(R_B + R_O) \quad (1)$$

The question then arises of what to do when either the A or B cation sites is shared by two or more species, one of which may even be a vacancy. The concept of an "average" tolerance factor derived from an "average" site size seems at first meaningless, as each A site in this case will either be occupied by Ce^{3+}, Sr^{2+}, or a vacancy, and not by an "average" cation; however, as the strains caused by each species will be averaged over the whole structure, it is not unreasonable to expect local relaxations to allow for the stabilization of an "average" structure. The further question of how to account for vacancies in the structure has been variously handled. In work by Ruiz et al.[20] on $La_{(2-x)/3}Na_xTiO_3$, for example, it was found that the degree of tilt decreased with an increased A-site vacancy concentration, thus suggesting that vacancies *increase* the average A-site size. This effect might be explained by the electrostatic repulsion of the oxygen anions surrounding the vacancy. More conventionally, an A-site vacancy would be treated as a dopant of radius zero, thus *decreasing* the average A-site size and increasing the tendency of oxygen octahedra to tilt. Indeed, such tilting was first explained[21] by the stabilizing effect of octahedra as they tilt in order to reduce the size of the cuboctahedral A-site which is occupied by a cation too small for the available volume. The onset of tilt transitions allows for steady thermal expansion with little modification of the octahedral volume.[22–25]

The tolerance factors of these compounds, if the vacancies were neglected, would be between 0.991 ($x = 0.4$) and 1.004 ($x = 0.1333$), indicating an untilted cubic structure. On the other hand, if the partial and mixed occupancy of the A-site is taken into account, these values would decrease to between 0.8905 ($x = 0.4$) and 0.9696 ($x = 0.1333$), consistent with the presence of a superlattice due to antiphase tilts such as that observed in Figure 2. As such a superlattice is largely constructed from tiny displacements of oxygen anions, and as XRD is insensitive to oxygen positions, neutron diffraction is required to unambiguously establish atomic positions.

All the compositions analyzed were very nearly ideal, as confirmed by EDS. Grains for which $0.1333 \leq x \leq 0.25$ looked relatively defect-free, and no second phase was observed; however, in the case of $x = 0.4$ grains were very defective. Streaks were visible in diffraction patterns and very faint ½{odd, even, even} β-reflections were observed in ⟨110⟩ patterns, usually indicative of antiparallel A-site cation displacements (Figure 5), which are not allowed in $R\bar{3}c$. As this composition corresponds to $Sr_{0.4}Ce_{0.4}TiO_3$, it is also possible that 1:1 cation ordering, also forbidden in $R\bar{3}c$, may be induced, lowering the symmetry still further. These possibilities are currently being investigated.

On the basis of the structural arrangement derived from electron diffraction (Figure 2), neutron diffraction data were used to refine the unit cell parameters, atomic positions, and isotropic displacement parameters (IDPs) for the various

(12) Hayward, S. A.; Morrison, F. D.; Redfern, S. A. T.; Salje, E. K. H.; Scott, J. F.; Knight, K. S.; Tarantino, S.; Glazer, A. M.; Shuvaeva, V.; Daniel, P.; Zhang, M.; Carpenter, M. A. *Phys. Rev. B* **2005**, *72*, 054110.
(13) Norby, P.; Krogh Andersen, E.; Andersen, N. H. *J. Solid State Chem.* **1995**, *119*, 191.
(14) Quo, Y.-Q.; Zhang, X.-H.; Waeppling, R. *J. Alloys Compd.* **2000**, *306*, 133.
(15) Yang, J.; Ma, Y. Q.; Zhang, R. L.; Zhao, B. C.; Ang, R.; Song, W. H.; Sun, Y. P. *Solid State Commun.* **2005**, *136*, 268.
(16) Nagabushana, B. M.; Sreekanth Chakradhar, R. P.; Ramesh, K. P.; Shivakumara, C.; Chandrappa, G. T. *Mater. Res. Bull.* **2006**, *41*, 1735.
(17) Howard, C. J.; Kennedy, B. J. J. *Phys.: Condens. Matter* **1999**, *11*, 3229.
(18) Lerch, M.; Boysen, H.; Hansen, T. *J. Phys. Chem. Solids* **2001**, *62*, 445.
(19) Kajitani, M.; Matsuda, M.; Hoshikawa, A.; Harjo, S.; Kamiyama, T.; Ishigaki, T.; Izumi, F.; Miyake, M. *Chem. Mater.* **2005**, *17*, 4235.
(20) Ruiz, A. I.; Lopez, M. L.; Pico, C.; Veiga, M. L. *J. Solid State Chem.* **2002**, *163*, 472.
(21) Reaney, I. M.; Colla, E. L.; Setter, N. *Jpn. J. Appl. Phys.* **1994**, *33*, 3984.
(22) Colla, E. L.; Reaney, I. M.; Setter, N. *Ferroelectrics* **1992**, *133*, 217.
(23) Colla, E. L.; Reaney, I. M.; Setter, N. *J. Appl. Phys.* **1993**, *74*, 3414.
(24) Colla, E. L.; Reaney, I. M.; Setter, N. *Ferroelectrics* **1994**, *154*, 35.
(25) Steiner, O.; Colla, E. L.; Reaney, I. M.; Setter, N. *Proceedings of the 'Third Euroceramics', Madrid*, European Ceramic Society, 1993; Vol. 2, p 223.

$Sr_{1-3x/2}Ce_xTiO_3$ ($x = 0.1333, 0.1667, 0.25, 0.4$) compositions in space group $R\bar{3}c$. Background coefficients, scale factors, profile functions, and sample absorption were also refined for a total of 17 parameters. In order to elucidate the arrangement and concentration of Sr and Ce, the Sr and Ce occupancies were also allowed to be refined. Table 1 summarizes the unit cell parameters and refinement results (displacement parameters) for each composition and temperature. The proportion of Ce^{4+} present was measured via X-ray photoelectron spectroscopy (XPS) in ref 1 and is included here in Table 1 for information. A charge-balance analysis of the refinement results agrees well with the XPS data, although there is a small anomaly in the charge balance for $x = 0.4$, which would actually suggest a negative amount of Ce^{4+}. This anomaly is undoubtedly the result of a structural change between $0.25 \leq x \leq 0.4$. The A-site bond valence sums decrease from 2.0273 at $x = 0.1333$ to 1.9029 for $x = 0.4$, while the Ti bond valence sums increase from 4.1736 at $x = 0.1333$ to 4.2258 at $x = 0.4$.

Figure 6 illustrates the observed and calculated neutron diffraction patterns for $Sr_{1-3x/2}Ce_xTiO_3$ ($x = 0.1333, 0.1667, 0.25, 0.4$). The arrowed peak in Figure 6b indicates a superlattice reflection at ≈2.35 Å corresponding to the same pseudocubic ½{311} also indicated by some of the α symbols in Figure 2b.

In this structure, the positions of the cations are fixed. There is only one degree of freedom (x), which is in the 18e oxygen positions. Ideally x = 0.5, and the size of the deviation away from 0.5 is related to the severity of octahedral tilting. Using the structure of the $Sr_{0.625}Ce_{0.25}TiO_3$ ($x = 0.25$) material, for which it was found that x = 0.5184, it can easily be calculated that the first visible XRD (Cu Kα) peak is at 22.86°, with the intensity ($I \sim 5.6\%$) corresponding to $(1\bar{0}2)$, $(11\bar{2})$, and (012) (the pseudocubic {100}). The first superlattice reflection to appear would be the extremely weak ½{311} peak at 38.38° ($I = 0.23\%$). All the other allowed superlattice peaks are so weak as to be nonexistent. Such peaks are virtually impossible to detect via conventional XRD, which is undoubtedly why they were not observed. The tilted structure is illustrated in Figure 7.

Using the calculated effective angles of tilt for these four compositions, it is possible to extrapolate to a composition for which tilt is zero, i.e., a cubic structure. The curve in Figure 8 shows the relationship between composition and tilt angle. The extrapolation is based on a third-order polynomial curve fit and indicates that the tilted superstructure should be lost only when $x \leq 0.05$.

Figure 9 shows the ToF neutron powder diffraction data for *d*-spacings between 1.8 and 2.8 Å for $Sr_{0.4}Ce_{0.4}TiO_3$ (solid curve) and $Sr_{0.75}Ce_{0.1667}TiO_3$ (dashed curve). The inset clearly shows the reasons for the relatively poor refinement of $Sr_{0.4}Ce_{0.4}TiO_3$ (GOF = 11.43) compared to the other three compositions. Indeed, two major differences are especially noticeable near the reflection at 1.95 Å. First, the high-resolution data shows without any doubt a doubling of the peak. Second, as indicated by an arrow, a weak reflection is observable at ≈1.9 Å. On the basis of these observations, various refinements have been attempted using related subgroups of $R\bar{3}c$. So far, the *Cmmm* space group has resulted in the best fit; however, this space group only explains the doubling of the peak at 1.95 Å and not the additional weak peak at ≈1.9 Å, as shown by the tick marks in Figure 9. Using the *Cmmm* space group, the refinement converges to $a = 7.7574(2)$ Å, $b = 7.7760(2)$ Å, and $c = 7.7501(2)$ Å as cell parameters. Such symmetry implies four different Sr/Ce mixed sites (0,0,0; ½,0,0; ½,0,½; 0,0,½) which could indicate an ordering between these two elements, as reported by Howard et al.[5] for $Sr_{1-3x/2}La_xTiO_3$; however, ordering was not refined using the metric of this unit cell.

Conclusions

Four compositions in the $Sr_{1-3x/2}Ce_xTiO_3$ homologous series, corresponding to $x = 0.1333$, 0.1667, 0.25, and 0.4, have been produced in a single-phase form and crystallographically characterized. While no superlattice can be observed via X-ray diffraction, both electron and neutron diffraction show evidence of a noncubic supercell caused by antiphase tilting of oxygen octahedra. The most likely space group is $R\bar{3}c$, corresponding to an $a^-a^-a^-$ tilt system. The only exception is $Sr_{0.4}Ce_{0.4}TiO_3$, which possesses an obviously noncubic symmetry but is not $R\bar{3}c$. For this composition, refinements using trigonal symmetry give only an average structure, which is nevertheless informative, especially regarding the degree of tilt, which certainly increases with increasing *x*. The "real" structure of $Sr_{0.4}Ce_{0.4}TiO_3$ is still under investigation and will be part of a separate publication. The corresponding tolerance factors are only in agreement with this structure if the A-site vacancies are included in the calculations as dopants of radius zero.

Acknowledgment. This work has been supported by the National Science Foundation through the Major Research Instrumentation Program, Award 0521315.

Supporting Information Available: CIF files for $Sr_{1-3x/2}Ce_xTiO_3$ ($x = 0.1333, 0.1667, 0.25, 0.4$). This material is available free of charge via the Internet at http://pubs.acs.org.

CM703659F